Austrian Journal of Earth Sciences | Vienna | 2024 | Volume 117 | 45–49 | DOI: 10.17738/ajes.2024.0004

Natrochalcite $NaCu_2(SO_4)_2 \cdot H_3O_2$ from the Lavrion Mining District – a brief characterisation

Gerald Giester[1*] and Branko Rieck[1]

[1)] Department of Mineralogy, University of Vienna, Josef-Holaubek-Platz 2, 1090 Wien, Austria;

[*)] Corresponding author: gerald.giester@univie.ac.at

Keywords: natrochalcite, $NaCu_2(SO_4)_2 \cdot H_3O_2$, Lavrion, crystal structure, hydrogen bonding

Abstract

Recently, samples of natrochalcite, $NaCu_2(SO_4)_2 \cdot H_3O_2$, were discovered from the Esperanza Mine, Lavrion Mining District, Greece. In the present study this material is characterized by single crystal X-ray diffraction at ambient and LT conditions. Natrochalcite is monoclinic, space group *C*2/*m*, with $a = 8.809(2)$, $b = 6.196(1)$, $c = 7.504(2)$ Å, $\beta = 118.56(3)°$, $V = 359.7(1)$ Å^3, $Z = 2$, $R1 = 0.0195$ at room temperature. No symmetry change was observed down to 100K.

1. Introduction

The geology of Attica, Greece, comprises Alpine basement rocks, both metamorphic and non-metamorphic, and post-Alpine sediments (Tavoularis et al., 2021). The Lavrion area corresponds to the western part of the Attic-Cycladic metamorphic belt, in the back-arc region of the active Hellenic subduction zone (Voudouris et al., 2021).

The Lavrion Mining District is one of the most prolific mineral producing areas on a worldwide scale. Natrochalcite was only recently discovered there (Rieck et al., 2018) but has been known from other localities for over a century. By volume, the vast majority of natrochalcite has been found in Chile in the Chuquicamata Mine, but also the Fortuna mine, east of Baquedano, and the Bella Santiaguina and Lomas Bayas mines, Sierra Gorda, southwest of Calama, Antofagasta have produced significant quantities. At the other known localities (Mount Vesuvius, the Vallone Stope on the island of Elba, both in Italy, and the Empire Mine in Arizona, USA) natrochalcite was only found in tiny amounts.

Natrochalcite, $NaCu_2(SO_4)_2(OH)(H_2O)$, was described by Palache and Warren (1908) as a new mineral from Chuquicamata near Calama, Antofagasta, Chile; Palache (1939) verified the monoclinic symmetry. The crystal structure was determined by Rumanova and Volodina (1958) in space group *C*2/*m*, with Z = 2, suggesting the existence of a strong hydrogen bond with a short O-O contact of ~2.42 Å. The structure was refined on synthetic material (Giester and Zemann, 1987; Chevrier et al., 1993) and on natrochalcite from the Santiaguina mine, Sierra Gorda, southwest of Calama (Giester, 1989). Chemical analyses showed that sodium can be replaced by potassium in small amounts.

Potassium-dominant samples $KCu_2(SO_4)_2(OH)(H_2O)$ from fumaroles of the Great Fissure eruption, Tolbachik volcano, Kamchatka, Russia were described by Pekov et al. (2014) and the name kaliochalcite was given for the new mineral species. Substitution of potassium by calcium and sodium was only observed in negligible amounts.

To investigate the interesting hydrogen bond system with very short O-O contacts, natrochalcite and related compounds were examined by neutron diffraction (Chevrier et al., 1990, 1993) as well as by FTIR spectroscopy (Beran et al., 1997). In-situ high-pressure single-crystal X-ray diffraction studies (Ende et al. 2019) were carried out up to 10 GPa.

Among minerals, the structure type is further known for tsumcorite, $Pb(Zn,Fe^{3+})_2(AsO_4)_2(OH)(H_2O)$ (Tillmanns and Gebert, 1973). The tsumcorite group represents a series of complex arsenate, phosphate, sulphate, and vanadate species with the general formula $AM1M2(XO_4)_2Y$ (A = Ca, Pb, Na, K, Bi; M = Cu, Zn, Fe^{3+}, Co, Ni, Mg, Mn^{3+}; X = As, P, V; Y = $(OH)(H_2O)$ resp. H_3O_2, $(OH)_2$, $(H_2O)_2$), the space-group symmetry is *C*2/*m* (Z = 2) in most cases.

2. Material and methods

Natrochalcite from the Lavrion Mining District was first described by Rieck et al., (2018) in the Esperanza Mine, Kaminiza Area, Greece. The discovery was made in the ancient parts of the mine in an area close to the type localities of katerinopoulosite (Chukanov et al., 2018) and katsarosite (Giester et al., 2023). The natrochalcite samples (Figs. 1, 2) were all uncovered by dissolving thick crusts of chalcanthite overlaying antlerite. In small areas, natrochalcite occurs in place of or alongside antlerite. Relict chalcopyrite and bournonite are present in the marble matrix of the samples. It is possible that by careful examination of the treated material as described, additional specimens recovered from the general area of the mine could be found. The crystals are pyramidal-shaped with dominant form {111}. {110} is generally well developed, but the faces of the remaining forms are usually small and often not present in their complete complement. The color is pale green to yellow-green.

A chip of natrochalcite, 0.04 × 0.04 × 0.06 mm^3 in size, selected for homogeneous extinction, was mounted on a glass capillary with silicone grease. Room temperature (RT) single crystal X-ray diffraction data were obtained on an Enraf Nonius KappaCCD diffractometer, sealed tube, equipped with a graphite monochromator and monocapillary optics using Mo-K_α (λ = 0.71073 Å) radiation. Several sets of phi- and omega-scans with a scanwidth of 2° were combined at a crystal-detector distance of 35 mm to obtain corresponding full sphere data up to to 80° 2θ. Data processing with integration and absorption correction by evaluating multi-scans was done with the Enraf Nonius software package (1999). Additional single-crystal diffraction studies at 200 and 100 K were performed using a Bruker APEXII diffractometer equipped with a CCD area detector, an Incoatec Microfocus Source IμS (30 W, multilayer mirror, Mo-K_α) and a Cryostream 800 Plus LT device from Oxford Cryosystems. The structures were refined by least-squares techniques using the SHELXL program (Sheldrick, 2015) implemented in the shelXle GUI tool (Hübschle et al., 2011). Non-hydrogen atoms were refined with independent anisotropic displacement parameters. The atom labelling scheme was chosen in accordance with Giester and Zemann (1987).

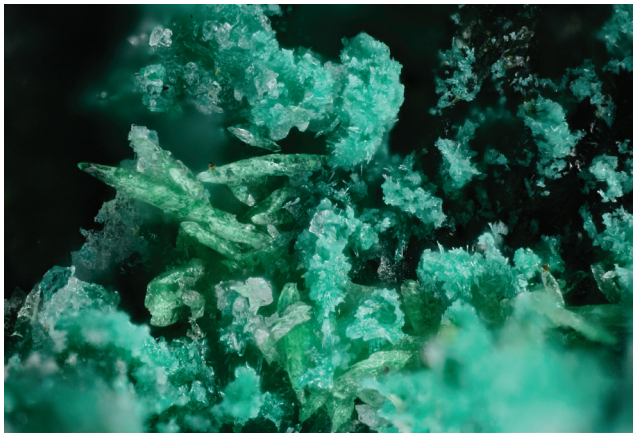

Figure 1: Typical elongated, pale green, striated crystals of natrochalcite with very thin, prismatic antlerite. FOV: 2.6 mm. Collection B. Rieck. Photo by H. Schillhammer.

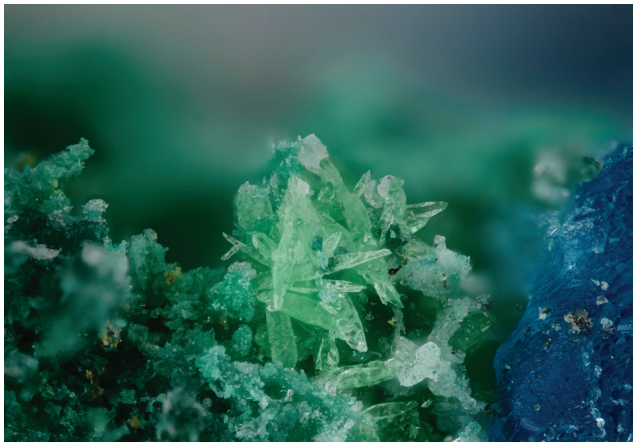

Figure 2: Green, steeply pyramidal crystals of natrochalcite with thin needles of blue-green antlerite and blue chalkanthite. FOV: 2 mm. Collection B. Rieck. Photo by H. Schillhammer.

The EDX analysis performed on a Zeiss EVO 40 XVP equipped with a Zeiss SmartEDX (30 mm^2 Silicon Drift Detector, Si_3N_4-Window) resulted in no other elements above detection limits than those expected. The average of 9 spot-analyses (20 kV and 7 nA for 60 seconds, count rate of 15k cps) was SO_3 42.49%, CuO 42.23%, Na_2O 8.17%, and H_2O (by difference) 7.11%. The ideal composition requires SO_3 42.45%, CuO 42.17%, Na_2O 8.22%, and H_2O 7.16%.

3. Results

The crystallographic data as well as details of the measurements and refinements are listed in Table 1, supplemented by a comparison with data in the literature. For the measurement at ambient conditions, the atomic coordinates are compiled in Table 2 and selected interatomic distances and angles in Tables 3 and 4. Further details of the crystal structure investigation can be obtained from the joint CCDC/FIZ Karlsruhe online deposition service: https://www.ccdc.cam.ac.uk/structures/ by quoting the deposition numbers 2320986 (RT), 2320987 (200 K), and 2320988 (100 K).

4. Discussion

The crystal structure of natrochalcite is characterized by infinite chains (Fig. 3) along [010], which consist of edge-sharing CuO_6 octahedra. This [4+2] coordination is Jahn-Teller distorted, as often observed for divalent copper. The chains are linked to SO_4 tetrahedra via common corners to form sheets parallel (001). The sodium atoms, located in-between at *z/c* = 0.5, are coordinated to 8 oxygen ligands. These distorted NaO_8 cubes share edges and corners with adjacent CuO_6 and SO_4 groups to build a framework (Fig. 4). In addition, a system of very strong

Crystal Data	RT	200 K	100 K	Chile[1]	Synth.[2]
space group	*C*2/*m*	*C*2/*m*	*C*2/*m*	*C*2/*m*	*C*2/*m*
a (Å)	8.809(2)	8.787(2)	8.777(2)	8.812(2)	8.809(1)
b (Å)	6.196(1)	6.177(1)	6.169(1)	6.188(2)	6.187(1)
c (Å)	7.504(2)	7.482(2)	7.471(2)	7.510(2)	7.509(1)
β (°)	118.56(3)	118.59(1)	118.57(1)	118.70(1)	118.74(1)
V (Å^3)	359.7(1)	356.6(1)	355.3(1)	359.2(1)	358.9(1)
Z	2	2	2	2	2
ρ_{calc} (g cm^{-3})	3.483	3.513	3.526		
μ (MoKα) (mm^{-1})	6.6	6.7	6.7		
unique data	1180	1200	1195		
data with $F_o>4\sigma(F_o)$	1111	1142	1135		
variables	51	51	51		
R1 [for $F_o>4\sigma(F_o)$] [3]	0.019	0.015	0.014		
*wR*2 [for all F_o^2] [3]	0.050	0.041	0.040		
a, b [3]	0.022, 0.38	0.020, 0.23	0.020, 0.30		
$\Delta\rho_{min\ /\ max}$ (eÅ^{-3})	-0.8 / 1.3	-0.7 / 0.5	-0.8 / 0.5		

Table 1: Crystal data and details of the intensity measurement and structure refinements for natrochalcite from Lavrion at various temperatures and a comparison with data in literature
[1] = Giester (1989); [2] Giester and Zemann (1987);
[3] $R1 = \Sigma F_o - F_c / \Sigma F_o$; $wR2 = [\Sigma w(F_o^2 - F_c^2)^2 / \Sigma w(F_o^2)^2]^{½}$; $w = 1 / [\sigma^2(F_o^2) + (a\times P)^2 + b\times P]$; $P = \{[\text{max of } (0 \text{ or } F_o^2)] + 2F_c^2\} / 3$

	x	*y*	*z*	$U_{iso/eq}$	U^{11}	U^{22}	U^{33}	U^{23}	U^{13}	U^{12}
Na	0	0.5	0.5	0.0240(2)	0.0138(4)	0.0359(7)	0.0176(4)	0	0.0038(4)	0
Cu	0.25	0.25	0	0.00863(6)	0.00669(8)	0.00708(8)	0.01071(8)	-0.00110(5)	0.00303(6)	0.00042(4)
S	0.09096(4)	0	0.30091(5)	0.00737(6)	0.00604(11)	0.00796(12)	0.00728(12)	0	0.00253(9)	0
O1	0.19351(15)	0	0.19136(18)	0.01354(18)	0.0145(4)	0.0140(5)	0.0174(5)	0	0.0119(4)	0
O2	0.20844(16)	0	0.51705(16)	0.0159(2)	0.0150(4)	0.0188(5)	0.0077(4)	0	0.0005(3)	0
O3	-0.02005(9)	0.19663(13)	0.24342(12)	0.01182(12)	0.0090(3)	0.0088(3)	0.0147(3)	0.0000(2)	0.0033(2)	0.0016(2)
OH	0.15748(13)	0.5	0.07523(15)	0.00848(15)	0.0072(3)	0.0088(4)	0.0093(4)	0.000	0.0039(3)	0.000
H1	0.037(3)	0.5	-0.002(11)	0.05(2)						
H2	0.206(4)	0.5	0.210(3)	0.036(9)						

Table 2: Atomic coordinates and displacement parameters of natrochalcite with e.s.d.'s in parentheses, RT measurement. H1 half-occupied.

and intermediate hydrogen bonds (Tab. 4) strengthens the structure. This formal centrosymmetric arrangement can be described as disordered $(H_2O)(OH)^{1-}$ or $(H_3O_2)^{1-}$, for a detailed discussion see (Chevrier et al., 1990, 1993).

Low temperature data down to 100K do not indicate any symmetry change of the natrochalcite structure; the short OH---OH hydrogen bond is moderately reduced from 2.445 Å (RT) to 2.433 Å (100K), the longer contact OH---O2 from 2.702 Å (RT) to 2.681 Å (100K). The bond lengths distortion of the NaO_8 polyhedron decreases at lower temperatures. Contrary, HP (up to 10 GPa) single-crystal X-ray diffraction studies (Ende et al., 2019), supplemented by Raman spectroscopic data, indicate lowered symmetry at elevated pressure above 2 GPa. Due to the preserved *C*-centring only two space groups are reasonable then, *Cm* (no. 8) and *C*2 (no. 5). Unit cell volumes are reduced (from ambient conditions to 10 GPa) in the range 360 to 320 Å^3.

Chemical analysis of natrochalcite from Lavrion proves a rather ideal composition without significant replacement of sodium or copper by other elements. This is also reflected in a unit-cell volume that is close to the one of the pure synthetic compound (see Tab. 1).

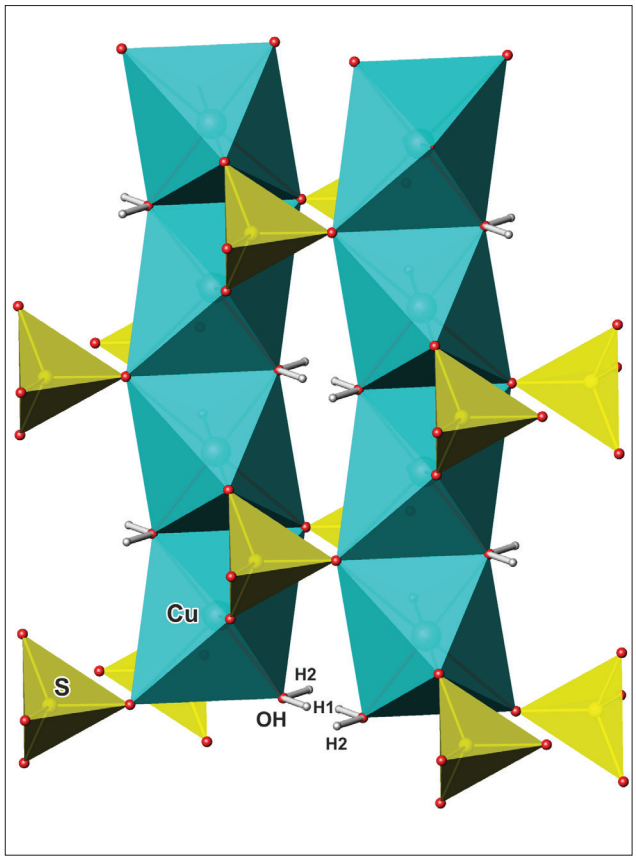

Figure 3: Structure detail of natrochalcite with chains along [010], formed by shared edges of CuO_6 octahedra (blue), further cornerlinked via SO_4 tetrahedra (yellow) to sheets parallel (001). Structure drawings were done with Atoms (Dowty, 2016).

		RT	200K	100K	v
Cu–OH	2×	1.9550(7)	1.9506(5)	1.9490(5)	0,47
Cu–O3	2×	2.0027(12)	2.0002(6)	2.0010(6)	0,42
Cu–O1	2×	2.3221(9)	2.3137(6)	2.3072(6)	0,17
<Cu–O> /Σv		**2,093**	**2,088**	**2,086**	**2,13**
Na–O1	2×	2.5835(17)	2.5876(10)	2.5956(9)	0,12
Na–O2	2×	2.6318(14)	2.6117(10)	2.5965(9)	0,11
Na–O3	4×	2.6355(9)	2.6153(7)	2.6031(6)	0,1
<Na–O> / Σv		**2,622**	**2,607**	**2,6**	**0,88**
S–O2		1.4480(13)	1.4484(9)	1.4500(9)	1,61
S–O1		1.4839(12)	1.4833(9)	1.4844(8)	1,46
S–O3	2×	1.4910(8)	1.4914(7)	1.4923(6)	1,43
<S–O> / Σv		**1,478**	**1,479**	**1,48**	**5,94**

Table 3: Selected interatomic bond lengths (Å) for natrochalcite at RT, 200K and 100K; bond valences < (v.u.) (Brese and O'Keeffe, 1991) are calculated for RT data.

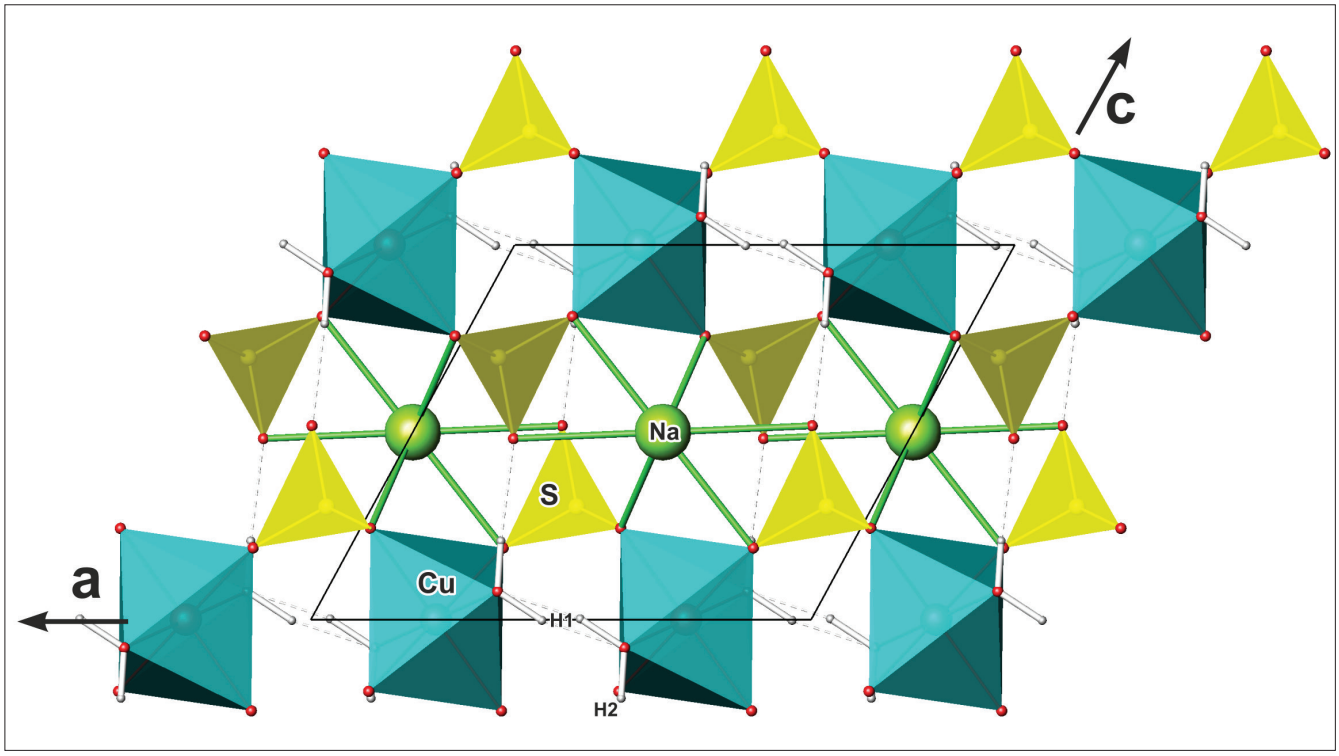

Figure 4: Crystal structure of natrochalcite projected onto (010), illustrating further package by NaO_8 polyhedra (Na atoms in green) and hydrogen bonding.

	D–H (Å)			D–A (Å)			D–H···A (°)			H1–OH–H2 (°)		
	RT	200K	100K	RT	200K	100K	RT	200K	100K	RT	200K	100K
OH–H1···OH	0.93(2)	0.93(2)	0.93(3)	2.445(2)	2.436(2)	2.433(2)	165(9)	169(9)	167(8)			
OH–H2···O2	0.89(2)	0.88(2)	0.89(3)	2.702(2)	2.688(1)	2.681(2)	177(3)	180(3)	176(3)	119(6)	115(6)	118(6)

Table 4: Hydrogen bond system for natrochalcite at RT, 200K and 100K.

5. Conclusions

Natrochalcite from the Lavrion deposit, Greece, has been studied in detail for the first time using single crystal X-ray diffraction at ambient conditions and low temperatures. The results of previous crystal structure determinations were verified; possible phase transformations at low temperatures down to 100 K were not observed. The chemical composition is close to the ideal formula, without any significant incorporation of other elements.

Acknowledgements

Mr. H. Schillhammer is warmly thanked for providing the photographs of the natrochalcite specimens. Positive comments from two anonymous reviewers are kindly acknowledged.

References

Beran, A., Giester, G., Libowitzky, E., 1997. The hydrogen bond system in natrochalcite-type compounds – an FTIR spectroscopic study of the $H_3O_2^-$ unit. Min Petr. 61, 223–235.

Brese N.E., O'Keeffe, M., 1991. Bond-Valence Parameters for Solids. Acta Crystallogr. B 47, 192–197.

Chevrier, G., Giester, G., Jarosch, D., Zemann, J., 1990. Neutron diffraction study of the hy-drogen-bond system in $Cu_2K(H_3O_2)(SO_4)_2$. Acta Crystallogr., C46, 175–177.

Chevrier, G., Giester, G., Zemann, J., 1993. Neutron refinements of $NaCu_2(H_3O_2)(SO_4)_2$ and $RbCu_2(H_3O_2)(SO_4)_2$. Variation of the hydrogen bond system in the natrochalcite-type series. Z Kristallogr., 206, 7–14.

Chukanov, N.V., Pekov, I.V., Belakovskiy, D.I., Britvin, S.N., Stergiou, V., Voudouris, P., Magganas, A., 2018. Katerinopoulosite, $(NH_4)_2Zn(SO_4)_2{\cdot}6H_2O$, a new mineral from the Esperanza mine, Lavrion, Greece. European Journal of Mineralogy 30/4, 821–826.

Dowty, E., 2016. ATOMS for Windows V6.5.0, *Shape Software*, 521 Hidden Valley Road, Kingsport, TN 37663 USA.

Ende, M., Giester, G., Kurz, M., Miletich, R., 2019. Symmetry lowering in natrochalcite $NaCu_2(H_3O_2)(SO_4)_2$ under pressure. Acta crystallographica, 2019, Vol.75, p.E300-E300.

Enraf Nonius, 1999. Kappa CCD Program Package: COLLECT, DENZO, SCALEPACK, SORTAV, Nonius BV, Delft, The Netherlands.

Giester, G., 1989. The crystal structures of $Ag^+Cu_2(OH)(SO_4)_2{\cdot}H_2O$ and $Me^+Cu_2(OH)(SeO_4)_2{\cdot}H_2O$ [Me^+=Ag,Tl,NH_4], four new representatives of the natrochalcite type, with a note on natural natrochalcite. Z Kristallogr., 187, 239–247.

Giester, G., Rieck, B., Lengauer, C.L., Kolitsch, U., Nasdala, L., 2023. Katsarosite $Zn(C_2O_4){\cdot}2H_2O$, a new humboldtine-group mineral from the Lavrion Mining District, Greece. Miner Petrol. 117, 259–267.

Giester, G., Zemann, J., 1987. The crystal structure of the natrochalcite-type compounds $Me^+Cu_2(OH)(zO_4)_2{\cdot}H_2O$ [Me^+=Na,K,Rb; z=S,Se], with special reference to the hydrogen bonds. Z Kristallogr. 179, 431–442.

Hübschle, C.B., Sheldrick G.M., Dittrich B., 2011. ShelXle: a Qt graphical user interface for SHELXL. J. Appl. Cryst., 44, 1281–1284.

Palache, C., 1939. Kroehnkite and natrochalcite from Chile. American Journal of Science, July 1939, 237/7, 447–455.

Palache, C., Warren, C.H., 1908. Kröhnkite, natrochalcite (a new mineral), and other sulphates from Chile. American Journal of Science, 26, 342–348.

Pekov, I.V., Siidra, O.I., Chukanov, N.V., Yapaskurt, V.O., Belakovskiy, D.I., Murashko, M.N., Sidorov, E.G., 2014. Kaliochalcite, $KCu_2(SO_4)_2[(OH)(H_2O)]$, a new tsumcorite-group mineral from the Tolbachik volcano, Kamchatka, Russia. European Journal of Mineralogy, 26, 597–604.

Rieck, B., Kolitsch, U., Voudouris, P., Giester, G., Tzeferis, P., 2018. Weitere Neufunde aus Lavrion, Griechenland. Mineralien Welt, 29/5, 32–77.

Rumanova, I.M., Volodina, G.F., 1958. The crystal structure of natrochalcite $NaCu_2(OH)[SO_4]_2$ H20 = $Na[SO_4]_2[Cu_2,OH,H_2O]$. Dokl. Akad. Nauk SSSR, 123, 78–81 [in Russian].

Sheldrick, G.M., 2015. Crystal structure refinement with SHELXL. Acta Crystallogr. C71, 3–8.

Tavoularis, N., Papathanassiou, G., Ganas, A., Argyrakis, P., 2021. Development of the Landslide Susceptibility Map of Attica Region, Greece, Based on the Method of Rock Engineering System. Land, 10, 148.

Tillmanns, E., Gebert, W., 1973. The crystal structure of tsumcorite, a new mineral from the Tsumeb mine, S. W. Africa. Acta Crystallogr., B29, 2789–2794

Voudouris, P., Melfos, V., Mavrogonatos, C., Photiades, A., Moraiti, E., Rieck, B., Kolitsch, U., Tarantola, A., Scheffer, C., Morin, D., et al., 2021. The Lavrion Mines: A Unique Site of Geological and Mineralogical Heritage. Minerals, 11/1, 76.

Received: 11.01.2024
Accepted: 11.03.2024
Editorial Handling: Bastian Joachim-Mrosko